Novel Morphology of Polyethylene Crystals Created upon Melt Crystallization of Spin-Coated Film

Jie Wang, Guanghao Lu, Ligui Li, Zhihui Lu, Xiaoniu Yang,* and Enle Zhou

State Key Laboratory of Polymer Physics and Chemistry, Changchun Institute of Applied Chemistry, Chinese Academy of Sciences, Graduate School of the Chinese Academy of Sciences, Renmin Str. 5625, Changchun 130022, P. R. China

Received October 27, 2007; Revised Manuscript Received December 11, 2007

ABSTRACT: We demonstrate a strikingly novel morphology of high-density polyethylene (HDPE) crystal obtained upon melt crystallization of spin-coated thin film. This crystal gives windmill-like morphology which contains a number of petals. A detailed inspection on this morphology reveals that each petal is actually composed of terrace-stacked PE lamellae, in which the polymer chains within crystallographic $a-c$ planes adopt ~45° tilting around *b*-axis. The surrounding domains associated with a petal of the windmill composed of twisted lamellar overgrowths with an identical orientation of their long axis, which is the crystallographic *b*-axis shared by the petal and its corresponding twisted lamellar overgrowths. The parameters involving molecular structure of the materials, preparation history of the specimen, and subsequent crystallization conditions which possibly influence the formation of this novel morphology have been subsequently discussed. The acquisition of the new morphology of polyethylene crystal should be linked to the special thermodynamic history and large-scale uniformity of the thin film prepared via hot spin-coating method.

Introduction

Thin or ultrathin polymer films have received wide attention for their broad applications in many fields.[1−5] To achieve large-scale (ultra)thin polymer film, the solution-based film deposition technique is an ideal approach, among which spin-coating is the well-established method for preparing smooth polymeric coatings on flat substrates.[6−12] As one of the most widely used methods for thin film deposition, spin-coating has its unique advantages to achieve polymer film with large-scale dimensions up to tens of square centimeters, precisely controllable thickness, and smooth surface. From a thermodynamic point of view, because of its very fast solvent evaporation, the thus-obtained film however is frequently in an unstable (or metastable) state, which will transfer to a more stable state as the system gains enough energy to overcome the local barrier, for instance, upon thermal annealing. This process could be used to construct a new but more stable state having novel morphological features.[13]

The crystallization of synthetic polymers, and of polyethylene in particular, has been a subject of intensive study for more than half century.[14−17] It is natural that this semicrystalline polymer is the most intensively and thoroughly studied material and is always first exemplified to elucidate crystallization and morphology of the polymer. As one of the most successfully commercialized polymers, polyethylene could be found in a wide range from the packaging in everyone's kitchen to high-end applications. However, there are still many phenomena waiting for further understanding or clarification, in which crystallization and morphology form one of the most important aspects.

It is well-known that single crystals of polyethylene are commonly grown from dilute solution in xylene or other solvents.[16,18] Crystallization of polyethylene from its melt typically results in polycrystalline aggregations such as spherulites, axialites, or single crystals with lenticular shape, S shape, or others.[18−28] It is worthy of noting in such a case its morphology is frequently related to the film thickness as influenced by the surfaces or interfaces.[29,30] However, scarcely has study been devoted to elucidate the crystallization of polyethylene in a well-defined thin film with uniform thickness prepared via, for instance, spin-coating.[11] The main reason behind this might be no solvent so far has been found for preparing PE solution with enough concentration which could be used for thin film deposition via spin-coating at room temperature. In this work, we exhibit a strikingly new morphology of polyethylene as obtained from melt crystallization of initially spin-coated thin film. The formation of this novel morphology may be linked to both the nonthermodynamic state and large-scale uniformity of the thickness associated with the thin film prepared via spin-coating.

Experimental Section

Materials. The high-density polyethylene (HDPE) with partial substitute of butyl branches was kindly supplied by China Petroleum & Chemical Corp. The number-average molecular weight (M_n) and polydispersity distribution index (PDI) were determined to be 8.6 $\times$ 10^3 g/mol and 30.1, respectively, by gel permeation chromatography (GPC) (Waters 150C). ^{13}C nuclear magnetic resonance (NMR) measurements indicated the average number of butyl branches attached to the polymer chain is 5.1 per 1000 ethylene monomers. Note that the branch content only represents an average value. In order to show the independence of this unique morphology of polyethylene on this specific material source, other polyethylene samples with different molecular architecture, molecular weight, and distribution have been examined for comparison. Molecular structure, molecular weight, and its distribution for these polyethylene samples are listed in Table 1. If not specifically noted, all HDPE sample used in this work is referred to But-PE, although comparable morphology could be always observed from all these samples via slight adjustment of crystallization conditions, for instance, heating temperature or cooling rate.

Sample Preparation. All the original thin polyethylene films were prepared on the glass substrates via the spin-coating method. The substrates were carefully cleaned in a standard cleaning procedure, as first cleaned in turn by ultrasonic treatment in acetone, isopropanol, and ultrafiltered water (Milli-Q), blown-dry with

* Corresponding author. E-mail: xnyang@ciac.jl.cn.

10.1021/ma7023842 CCC: $40.75
Published on Web 01/25/2008

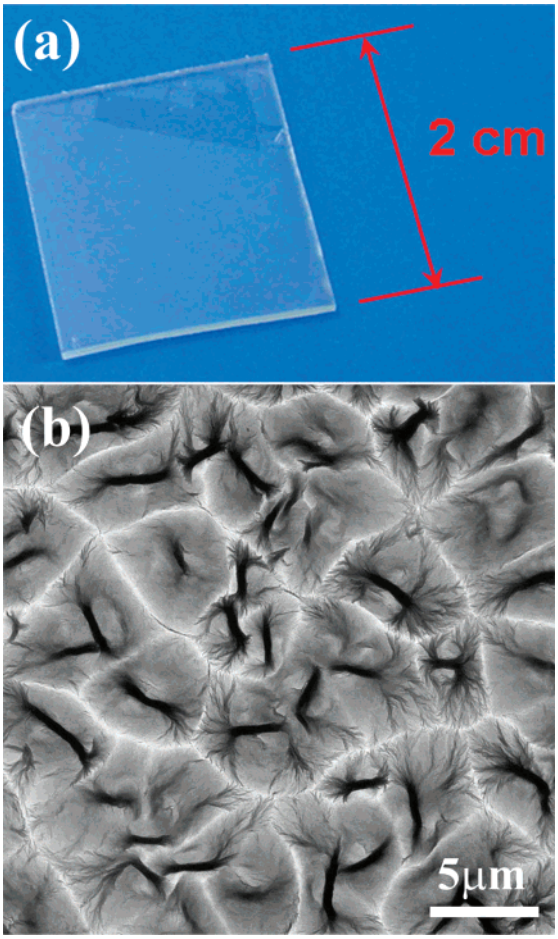

Figure 1. (a) Real image showing large scale (2 cm × 2 cm) homogeneous thin film of polyethylene with a thickness ca. 300 nm on a glass substrate prepared via hot spin-coating method. A portion of this thin film on upper-right corner has been transferred for the investigations. (b) Transmission electron micrograph showing typical morphology of the thin film.

Table 1. Molecular Structure, Molecular Weight, and Its Distribution of Polyethylene Samples Used in This Work

PE sample	M_n (g/mol)	PDI	branch substitute
But−PE	8.6×10^3	30.1	butyl (0.51 mol %)
Hex−PE	1.0×10^4	31.4	hexyl-1 (0.86 mol %)
MTT−PE	1.3×10^5	7.8	NO (but with 0.74% montmorillonite)
MAO−PE	8.7×10^4	2.3	NO

nitrogen, and finally treated with UV/ozone for 20 min. The polyethylene was dissolved in hot xylene to achieve the solution with a concentration of 10 mg mL^{-1}. All the necessary equipment (glass substrates, chucks, pipets, etc.) and the solution as well were preheated to the actual deposition temperature (e.g., 180 °C). The time used for transfer this preheated hot substrate from oven to spin-coater was controlled within 10 s. The typical rotation speed used in this work was 1000 rpm. As shown in Figure 1a, a very homogeneous thin PE film within an area of a few square centimeters is obtained via this method. Afterward, a small portion of the film was transferred to copper grids coated with a thin layer of amorphous carbon by using the flotation technique.

The crystallization of the specimen mounted on the carbon-coated copper grids was actually performed on a silver hot stage (Linkam THMS 600, made in England). After the cover had been fastened, the chamber was filled with dry nitrogen before heating. No nitrogen purge was provided during all the heating and crystallization process. If not specifically noted, the nonisothermal crystallization of the thin film was conducted by first heating the specimen to a given temperature and kept for ca. 10 min and then cooled to room temperature at 3 °C/min. Thus, the obtained specimen is then used for morphology investigations.

Instruments. Transmission electron microscopy (TEM) observation and selected-area electron diffraction (SAED) analysis were conducted by a JEOL JEM-1011 working on an accelerating voltage of 100 kV.

Atomic force microscopy (AFM) measurements were performed on SPA300HV with an SPI 3800 controller, Seiko Instruments Industry, Co. Ltd. The images were taken with tapping mode at room temperature.

Film thickness measurements were also performed with a Veeco DekTak 6M stylus profiler.

All the crystallization of the thin film specimens was performed on a silver hot stage (Linkam THMS 600, England). The temperature of this hot stage is controlled through a Linkam TMS 94 controller with a temperature variation within 0.1 °C.

Results and Discussion

1. Novel Morphology of Polyethylene Crystals. As shown in Figure 1a, the thin polyethylene film with thickness ca. 300 nm seems very homogeneous even within large-scale dimension (2 cm × 2 cm) as prepared via the hot spin-coating method. The semitransparent appearance of the film indicates polyethylene has partially crystallized even under such a fast solvent evaporation. Microscopically, this thin film is composed of immature PE spherulites (or axialite-like PE crystals), as revealed by TEM image shown in Figure 1b. It should be noted that the most pronounced feature of this morphology is the very thick branch associated with each spherulite, serving as the main framework of the spherulite. These very thick lamellae could be one of the main contributions to the novel morphology reported in this work. In contrast, the conventional PE spherulites prepared via other methods, for instance, drop-casting from the same solution, do not show this feature at all. The formation of the immature PE spherulite should be related to the very fast solvent evaporation during thin film deposition by using hot spin-coating, which turns out that well-dissolved PE chains in the hot solution are almost quenched to the solid state. Although HDPE is regarded as one of the polymers with the highest crystallization kinetics, its full crystallization process has been hampered during this preparation. Anyway, homogeneous nucleation is still allowed, and crystal growth is however severely suppressed. As a consequence, the whole film is predominated by the immature PE spherulites or even by bundlelike crystals as the initial stage of spherulites. It should be noted that the size of spherulites in the spin-coated film is quite small but homogeneous due to the simultaneous nucleation in such a sudden cooling process is predominant.

As this film is heated to 180 °C and then cooled to room temperature at a rate of 3 °C/min, we obtain a strikingly novel PE crystals in terms of morphology with windmill-like appearance. As shown by an overview of Figure 2a, these windmills are homogeneously distributed over the whole film as observed. Each windmill crystal is typically composed of 4−6 petals. Interestingly, each petal associated with the same windmill mostly adopts either edge-to-edge or back-to-back relation to its neighbor petal (Figure 2b). If a single petal is further zoomed in, as shown in Figure 2c, it is interestingly observed this petal is actually composed of lamellar crystals with terrace stacking. The in-situ selected-area electron diffraction pattern (SAED) (Figure 2d) reveals that at least two types of crystal (or crystal cluster) contribute to this pattern. After a detailed inspection on the selected area as marked by the circle in Figure 2c, it could be found that the surrounding domain of the petal is actually composed of twisted lamellar overgrowths with almost

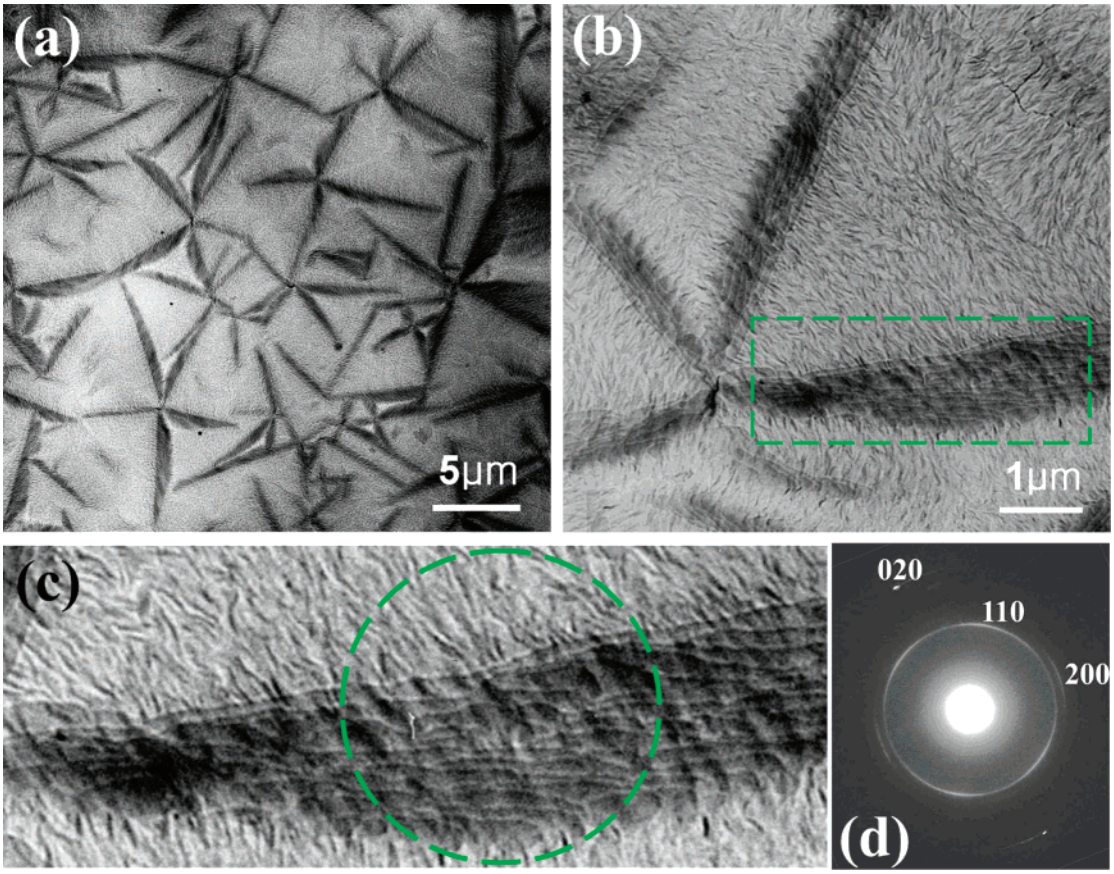

Figure 2. Bright-field (BF) TEM images of windmill-like polyethylene crystals obtained via melt crystallization upon melting at 180 °C and cooling to room temperature from its spin-coated thin film: (a) overview, (b) zoom-in of a windmill crystal, (c) further zoom-in of a petal, and (d) selected-area electron diffraction pattern from the marked area in (c).

the same orientation. Therefore, it is reasonable to ascribe those diffractions with arc shape, which could be indexed as the reflections from (110), (200), and (020) planes according to their *d*-spacing and orientation to the twisted lamellar overgrowths. Consequently, the additional very sharp diffraction spots also on arc (020) should be contributed from stacking lamellae of the petal. The appearance of only (020) reflections hints the tilting of PE chains in the lamellae relative to the normal to the film plane or the substrate and this tiling is most probably along crystallographic *b*-axis. It has been observed that *c*-axis (chain stems) of polyethylene frequently adopt a direction out of the normal to the lamellae surface, particularly for the crystals in the thin films. In the most cases, 5*k*l, 3*k*l, and 2*k*l instead of *hk*0 ($h \neq 0$) sets of reflections are typically observed as a consequence of the chain tilting of 30°, 46°, and 54°, respectively.[31] However, except for very clear (020) diffraction spots, no additional reflections associated with *hk*0 planes from the lamellae of the petal obtained in this work are observable.

In order to verify the assumption of not observed sets of reflections from *hk*0 ($h \neq 0$) planes to the tilting of PE chains within the lamellae and thus out of the incidence of electron beam, the tilting SAED experiments were carried out on the petal to acquire a diffraction pattern from crystallographic [001] axis. As hinted by the same orientation direction of (020) reflections from both twisted lamellar overgrowths (arc shape) and the lamellae of petal (spot shape), it could be affirmatively conclude that both types of lamellae roughly have the same orientation about crystallographic *b*-axis, which is along the growth direction of the twisted lamellar overgrowths. Therefore, by tilting the specimen along *b*-axis for around 45°, a diffraction pattern including all the sharp reflections from (110), (020), and (200) planes are obtained from the ideally aligned [001] axis. Figure 3 shows BF-TEM images of a windmill and SAED patterns on a petal both before (without) tilting (Figure 3a) and after a tilting along *b*-axis for 45° (Figure 3b). A schematic representation given in Figure 3c shows the orientation of folded polymer stems within the lamellae of both the petal and twisted lamellar overgrowths. As confirmed by the tilting SAED pattern, polyethylene chains in the lamellae of the petals adopt ca. 45° tilting relative to the normal to the lamellar surface along *b*-axis. The twisted lamellar overgrowths exactly beneath the petals should have the same orientation as that of the petals. Because of the twisting of these lamellar overgrowths, however, their molecular orientation changes along the growing direction.

As far as attention is paid to the relationship of the orientation between each petal of the windmill and its corresponding twisted lamellar overgrowths, as shown in Figure 4a, it seems the twisted lamellae associated with a single petal adopt an identical orientation and form a polygonal domain. The angle between the petal and the corresponding twisted lamellar overgrowths is roughly around 65°. More specifically, the angles from the straight edge of each petal to the long axis of the associated twisted lamellar overgrowths (as guided by the double-arrow lines) for a windmill are about 65° and its supplementary angle 115° alternately if observed in a fixed circular direction. We could present an even more convincing proof with respect to this interesting orientation of the petal relative to its corresponding twisted lamellae with an angle either 65° or supplement 115° between their neighbors. As shown in Figure 4b, this TEM image gives a petal with a crack and is thus partly split off after this petal has completed its growth, which could be confirmed by the continued feature of the stacked lamellae

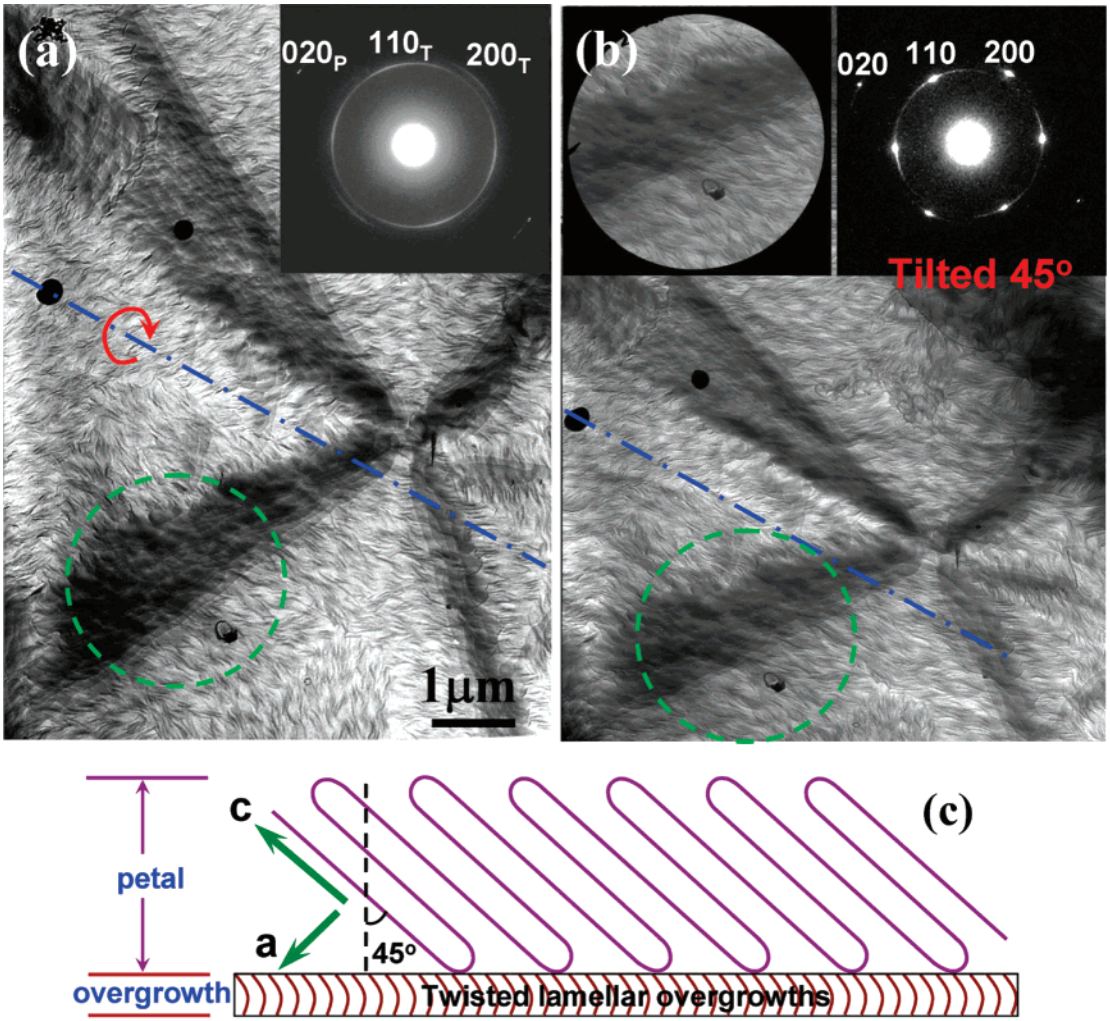

Figure 3. (a) BF-TEM image of a windmill crystal before tilting. The dash-dotted line and the curved arrow give tilting axis and direction, respectively. Inset is the SAED pattern, where diffractions indexed with subscription "P" are attributed to the petal and "T" twisted lamellar overgrowths. (b) BF-TEM image of the identical windmill after a 45° rotation about the axis indicated. Insets are the in-situ BF image (upper left) of the selected area and diffraction pattern (upper right). (c) Schematic representation showing the tilting orientation of PE chains in the petal with respect to both the twisted lamellar overgrowths and film plane.

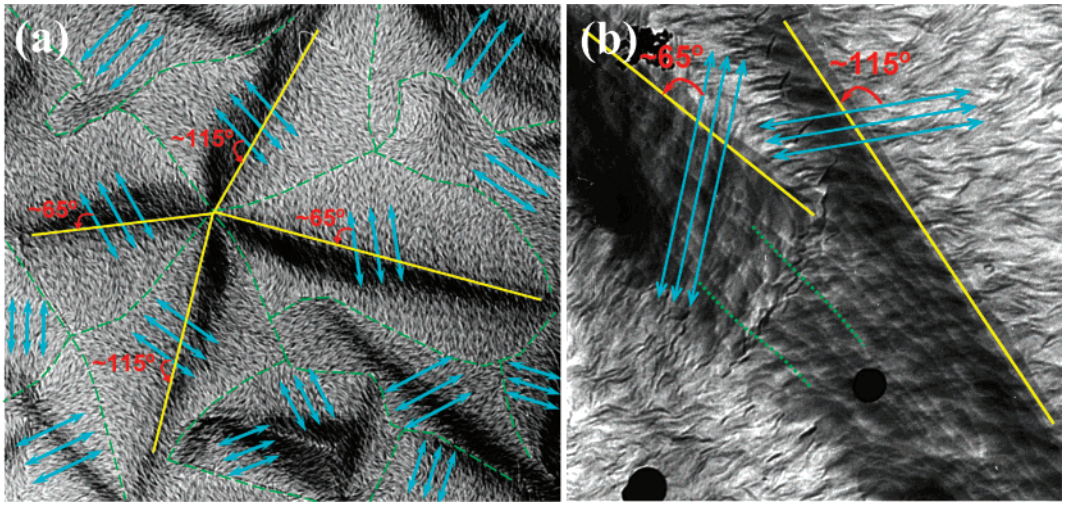

Figure 4. (a) TEM image showing the twisted lamellar overgrowths with a unique orientation associated with a petal form a polygonal domain. The angles from the straight edge of each petal to the corresponding long axis of the twisted lamellar overgrowths for a windmill are alternatively about 65° and its supplementary angle 115° in a fixed circular direction. (b) A crack and diverted growth direction of a petal and their corresponding twisted lamellar overgrowths.

before and after the crack, as marked by the dotted lines. The different angles (65° vs 115°) between the straight edge of the petal before and after cracking convictively disclose that the petals of the windmills form first toward their final dimension upon cooling cycle. The associated twisted lamellar overgrowths develop later, and their orientations are governed by the

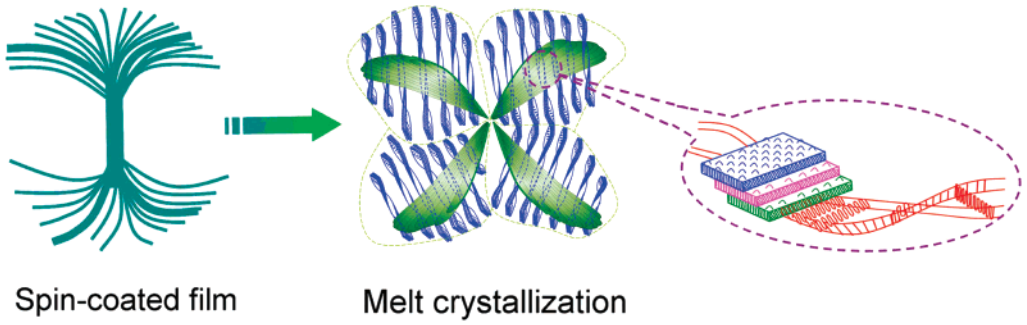

Figure 5. Schematic illustration demonstrating the main morphological feature of spherulitic crystal in spin-coated film, windmill crystal and the corresponding twisted lamellar overgrowths, and the formation detail of windmill as evolved from the spherulite upon melt crystallization.

corresponding petal. Since a windmill crystal reported here is at least composed of four petals, the predetermined crystal growth direction associated with each petal has to be preserved and be adopted for further growth due to the confinement by their neighbors within the thin film. By alternately taking 65° and 115° as the angle relative to the petal, the twisted lamellar overgrowths within the domain have minimized the angle with respect to their neighbor domains. However, we still cannot provide complete understanding of this specific angle, and further work is ongoing.

Figure 5 gives a schematic representation to demonstrate the formation of this novel polyethylene crystal. The spherulites with typical thick lamellae in the spin-coated film are regarded as the "forefather", in which nucleation starts and crystal growth continues during cooling process from the melt. Therefore, these petals crystallize first and actually guide the orientation of the twisted lamellar overgrowths which develops at a later stage. Because of twisting behavior of the lamellar overgrowths, the chain tilting does not stick to a fixed angle to the film plane anymore. In contrast, the pedals associated with the windmill crystals are composed of stacked—instead of twisted—lamellae, where polyethylene chains adopt 45° tilting along crystallographic *b*-axis. This chain tilting frequently leads to the bending or twisting morphology of the lamellae so as to reduce its unbalanced surface stress.[33−35] Keith et al. have also suggested that torsions of the PE lamellar crystals are also resulted from the unbalanced surface stresses in lamellae with favorable chain tilt.[36,37] However, the PE lamellae obtained in this work do not show any deformation like bending or twisting.[38] Instead, they adopt the morphology of terrace-dislocated overlapping of flat lamellae,[32,39] and thus deformation is prevented. This morphology could also serve as a manner to reduce the unbalanced surface stress through continuously dislocating the lamellae top to down.

2. Dependence of This Novel Morphology on the Crystallization Conditions, Sample History, and Types of Polyethylene. Heating Temperature. In order to disclose the origin and formation conditions for this unique windmill crystal, more relevant crystallization conditions had been examined. Since these crystals are typically achieved via crystallization from the melt, the highest heating temperature that the thin film experienced should play a key role in determining its morphology. As shown in Figure 6, these TEM images show the morphology of the specimens obtained via nonisothermal crystallization upon heating to different temperatures (ranging from 160 to 190 °C) and cooling to room temperature. All these samples are initially from the spin-coated film deposited on the same substrate. For the lowest temperature, 160 °C, the film almost demonstrates the typical spherulite morphology. However, a few petals are still resolvable from the micrograph (Figure 6a). As the temperature increased to 170 °C (Figure 6b), much more pronounced petals come out, which are already surrounded by the twisted lamellar overgrowths developed at later stage in the cooling cycle. If a higher temperature at 180 °C (Figure 6c) is applied, the crystals with windmill-like morphology become pronounce and appear everywhere within the film, as has already been demonstrated in Figure 2. For further increased temperature at 190 °C, these windmill crystals grow up by depletion more materials from their surroundings (Figure 6d). The even higher temperature will result in another type of morphology which will be reported elsewhere.

Morphology of the Initial Thin Film. Interestingly, these windmill crystals could not be obtained from conventionally prepared PE films even at the same crystallization atmosphere. As demonstrated by Figure 7, for the PE spherulites without obvious thick lamellae in the pristine film prepared via a typical drop-casting method (Figure 7a), only conventional spherulites (Figure 7b) could be obtained despite how the crystallization conditions have been adjusted. This confirms that those thick lamellae are necessary for obtaining these windmill crystals since it is very possibly that their nucleus have been partially preserved during heating process, which first nucleate and grow up into lamellae for the petals in the subsequent cooling process.

By combining the effects from both the heating temperature and the morphology of initial thin film on the morphology obtained, it could be easily drawn a conclusion that the formation of these unique crystals relies on two indispensable factors: one is the spherulites having very thick lamellae as prepared via spin-coating, and the other is the crystallization circumstance where these crystals develop. The formation of the windmills is associated with the partial preservation of nucleus in those thick lamellae with the assistance of surface air cooling effect during heating on a conventional hot stage. These preserved structures originally located in the thick lamellae will first nucleate and take priority for crystal growth and eventually develop into each petal of the windmill. As heating temperature goes higher, less nucleation sites could be kept and larger but less windmills are eventually achieved.

Types of Polyethylene Polymer. The polyethylene material we mainly used in this work is a type of HDPE with partial substitute of butyl branches. Then a question naturally arises whether this novel morphology is dependent on the unique molecular structure of this material. In order to exclude this influence and to show the independence of obtained novel PE crystals on the particular material, three other types of polyethylene have been examined. As shown in Figure 8, all these PE materials give similar windmill crystals via slightly changed or even the identical crystallization conditions. These specimens have covered types of PE samples with different substituted branches, butyl (But−PE) or hexyl (Hex−PE), and polymerized

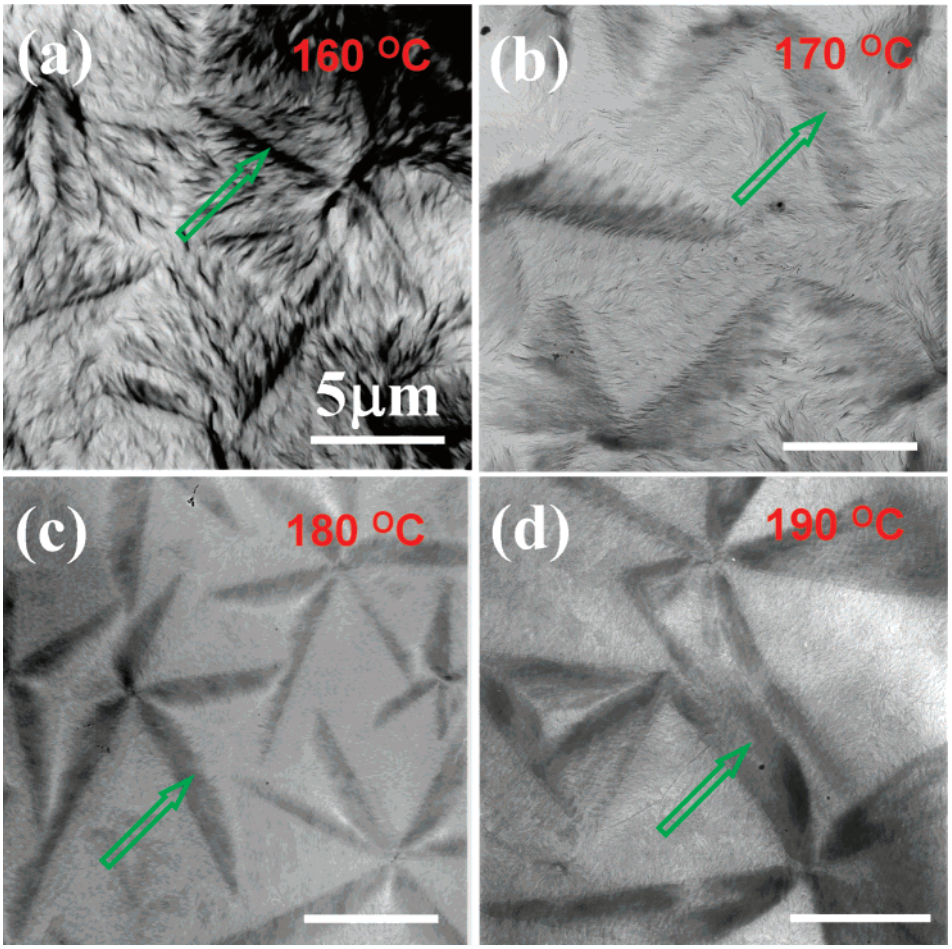

Figure 6. TEM images showing the morphological variations of windmill-like PE crystals obtained at different melting temperatures. The number at the upper left gives the melting temperature actually used. The arrows point out the different shape of the petals obtained at each temperature.

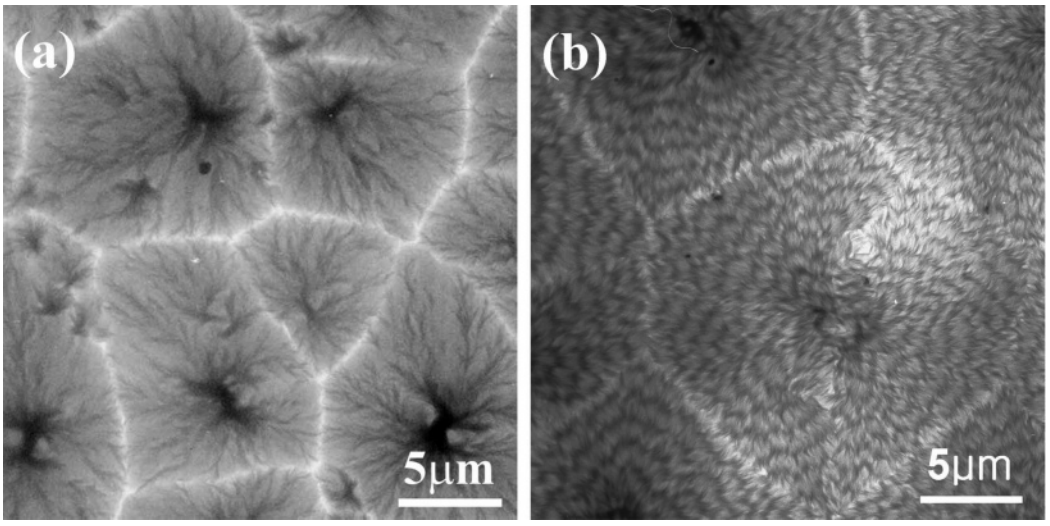

Figure 7. TEM images showing the dependence of windmill formation on the morphology of the initial film: (a) typical spherulites in the pristine PE film prepared via drop-casting and (b) conventional spherulites as obtained with the same conditions as that of Figure 2.

with different catalyst systems but without any substitute (MTT−PE and MAO−PE). The use of these specimens has also considered the variation of PDI with single molecular distribution, e.g., Hex−PE, MTT−PE, and MAO−PE, and with double molecular distributions, e.g., But−PE.

Crystallization Rate As Achieved by Cooling Rate. The formation of this novel morphology actually should be conducted during the cooling process after the specimen has been heated to a specific temperature. Anyone could have a question in mind whether the cooling rate also play a key role in determining the acquisition of this novel morphology. The most frequently used cooling rate in this work is 3 °C/min, which is already quite low compared to the frequently used cooling rate in polymer crystallization. However, even a low cooling rate

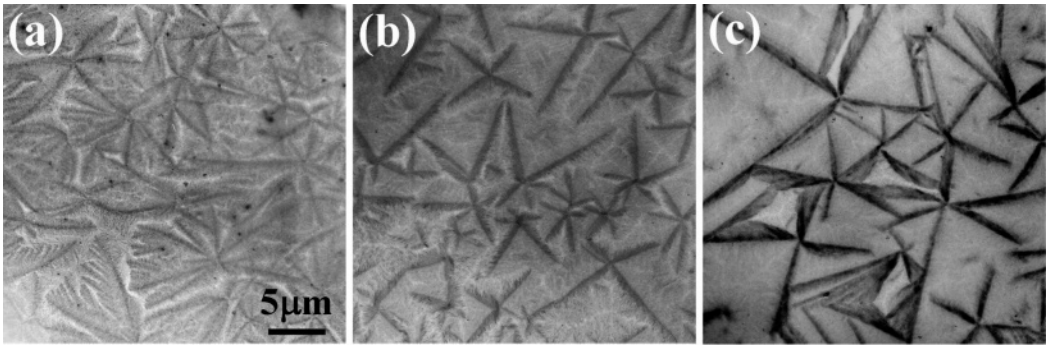

Figure 8. TEM images showing the dependence of windmill formation on the types of polyethylene materials: (a) MTT−PE, (b) MAO−PE, and (c) Hex−PE. All the specimens are prepared with the same conditions as that of Figure 2. All the images have the same scale bar.

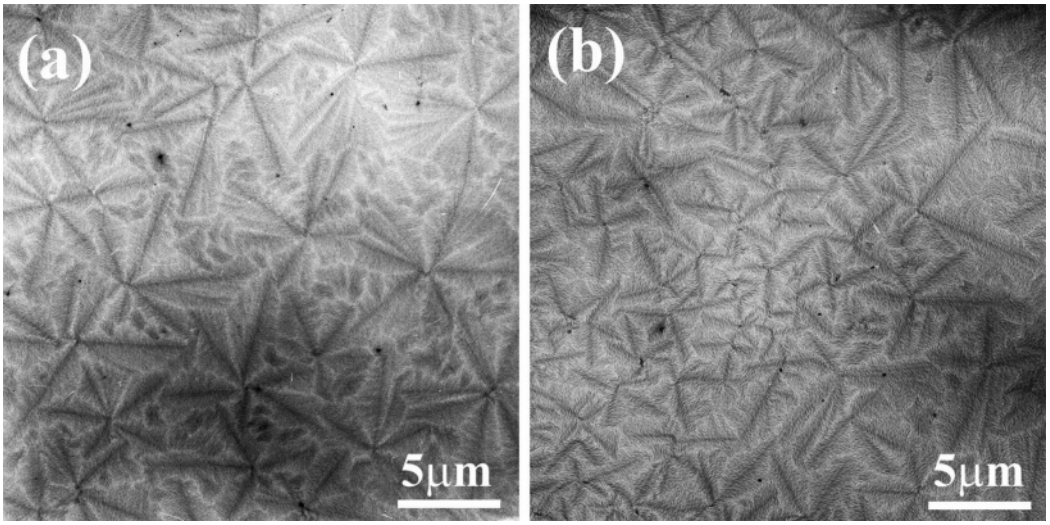

Figure 9. TEM images showing the dependence of the windmill formation on the cooling rate at (a) 100 and (b) 130 °C/min.

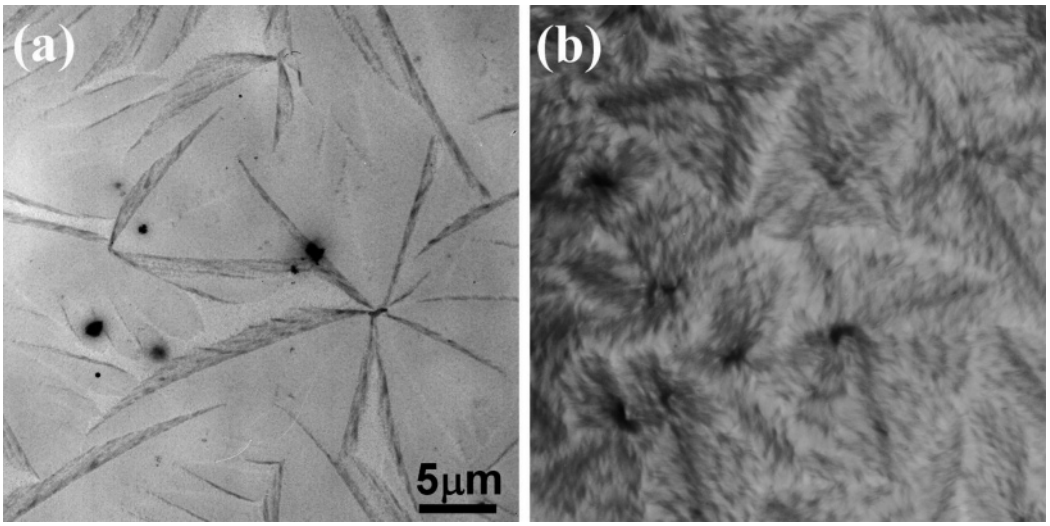

Figure 10. TEM images showing the dependence of the windmill formation on the thickness of the pristine film: (a) 150 and (b) 460 nm. Both images have the same scale bar.

at, e.g., 1 °C/min has also been used in this work, which successfully gives rise to this novel morphology. Therefore, we would like to divert our attention to examine how the highest cooling rate could still result in this morphology. Figure 9 shows the TEM images of the specimen prepared at very high cooling rate at 100 and 130 °C/min for parts a and b, respectively, which is the highest cooling rate within controllable capability of the hot stage used in this work. Overall, similar morphology has been obtained in the specimen prepared even via such a fast cooling process, although the size of the windmill become smaller as increased cooling rate and each petal looks more rough due mainly to the very fast crystallization process, which also hints that petals are formed at a higher temperature during the cooling cycle prior to the onset of the twisted lamellar

overgrowths. However, directly placing the melted specimen onto another hot stage which has been preset to a low-temperature results in conventional spherulites instead of this novel morphology. The sudden cooling process could be finished within a few second and thus an even higher cooling rate could be achieved. However, this operation also introduces a sudden air flow on the surface of the thin film specimen, which has negative effect on the formation of this novel morphology.

Thickness of the Film. As a novel morphology uniquely prepared from the thin film specimen, the film thickness should play a role in determining or at least have certain influence on the morphology obtained. As stated previously, the thickness of the pristine thin film used in this work is mostly around 300 nm, which is also the most suitable thickness to create this novel morphology. For those films with somewhat smaller or larger thickness, e.g., the thinner and thicker films of 150 and 460 nm, respectively, similar windmill crystals could still be constructed under the same crystallization condition and atmosphere. However, as shown in Figure 10, two predominant features of the windmills obtained have strong correlation with film thickness. First, the shape of the petals obtained from the thinner film (Figure 10a) is much more elongated than that from the thicker film. Second, the thicker film (Figure 10b) shows much pronounced backdrop composed of spherulitic crystals of polyethylene. As a consequence, the contrast of windmill crystals is rather low and a bit difficult to be recognized due to both the thick film and complicated background. In contrast, the backdrop of the thinner film is rather clean, which gives very pronounced petals. These results hint that the polymer material consumed to form these novel PE crystals are constraint to a certain amount at a given melting temperature and the remaining polyethylene material (if still have) will develop into twisted lamellar or even conventional spherulitic crystals, depending on the amount of material left after crystallization of windmill crystals.

Conclusions

In summary, we have shown a strikingly novel morphology of polyethylene with windmill-like appearance from an overview and each windmill comprising a number of petals. A detailed inspection on a petal shows it is composed of terraced-stacked lamellae, in which polyethylene chains adopt a unique $\sim 45°$ tilting around crystallographic *b*-axis. This morphology is typically achieved via melt crystallization of spin-coated thin film with uniform thickness.

We have also examined those parameters, e.g., molecular structure of the materials, preparation history of the thin film, and crystallization conditions, in order to form more specific conditions for obtaining this novel morphology. The success in preparation of windmill crystals from various types of polyethylene confirms this novel morphology is almost independent of a specific molecular structure of the polyethylene. However, a uniform-thickness film deposited via spin-coating and an appropriate melting temperature are necessary since the very thick lamella associated with the spin-coated film serves as nucleus during crystal development. The crystallization of these windmill crystals could be conducted within a very short time so that cooling rate has not that much influence on their formation. An appropriate thickness of the films is necessary for creating this novel crystal, and a film around 300 nm has been confirmed to be the most suitable thickness, although this value seems flexible somehow as a thinner film, e.g. 150 nm, or a thicker film, e.g. 460 nm, is still allowed.

Acknowledgment. This work was supported by National Fundamental Research Specific Foundation of China (Grant 2005CB623800). X.Y. thanks the Fund for Creative Research Groups (Grant 50621302) for financial support.

References and Notes

(1) Goffri, S.; Müller, C.; Stingelin-Stutzmann, N.; Breiby, D. W.; Radano, C. P.; Andreasen, J. W.; Thompson, R.; Janssen, R. A. J.; Nielsen, M. M.; Smith, P.; Sirringhaus, H. *Nat. Mater.* **2006**, *5*, 950.
(2) Frank, C. W.; Rao, V.; Despotopoulou, M. M.; Pease, R. F. W.; Hinsberg, W. D.; Miller, R. D.; Rabolt, J. F. *Science* **1996**, *273*, 912.
(3) Atashbar, M. Z.; Bejcek, B.; Vijh, A. *Sens. Actuators B* **2005**, *107*, 945.
(4) Davis, G. T.; Furukawa, T.; Lovinger, A. J.; Broadhurst, M. G. *Macromolecules* **1982**, *15*, 329.
(5) Lovinger, A. J.; Cais, R. E. *Macromolecules* **1984**, *17*, 1939.
(6) Bornside, D. E.; Macosko, C. W.; Scriven, L. E. *J. Imag. Technol.* **1987**, *13*, 122.
(7) Lawrence, C. J. *Phys. Fluids* **1988**, *31*, 2786.
(8) Despotopoulou, M. M.; Frank, C. W.; Miller, R. D.; Rabolt, J. F. *Macromolecules* **1996**, *29*, 5797.
(9) Bartczak, Z.; Argon, A. S.; Cohen, R. E.; Kowalewski, T. *Polymer* **1999**, *40*, 2367.
(10) Kressler, J.; Wang, C. *Langmuir* **1997**, *13*, 4407.
(11) Mellbring, O.; Kihlman Øiseth, S.; Krozer, A.; Lausmaa, J.; Hjerberg, T. *Macromolecules* **2001**, *34*, 7496.
(12) Wirtz, A. C.; Hofmann, C.; Groenen, E. J. J. *J. Phys. Chem. B* **2006**, *110*, 21623.
(13) Cheng, S. Z. D.; Lotz, B. *Polymer* **2005**, *46*, 8662.
(14) Keller, A. *Philos. Mag.* **1957**, *2*, 1171.
(15) Keller, A. *Faraday Discuss. Chem. Soc.* **1979**, *68*, 45.
(16) Bassett, D. C. *Principles of Polymer Morphology;* Cambridge University Press: New York, 1981.
(17) Hoffman, J. D.; Frolen, L. J.; Ross, G. S.; Lauritzen, J. I. *J. Res. Natl. Bur. Stand. A: Phys. Chem.* **1975**, *79A*, 671.
(18) Geil, P. H. *Polymer Single Crystals;* Interscience Publishers: New York, 1963.
(19) Organ, S. J.; Keller, A. *J. Polym. Sci., Polym. Phys. Ed.* **1986**, *24*, 2319.
(20) Keith, H. D. *J. Appl. Phys.* **1964**, *35*, 3115.
(21) Toda, A. *Polymer* **1990**, *32*, 771.
(22) Keith, H. D. *J. Polym. Sci.* **1955**, *17*, 291.
(23) Keith, H. D.; Padden, F., Jr. *J. Polym. Sci.* **1959**, *39*, 101.
(24) Toda, A. *Colloid Polym. Sci.* **1992**, *270*, 667.
(25) Toda, A.; Keller, A. *Colloid Polym. Sci.* **1993**, *271*, 328.
(26) Bassett, D. C.; Olley, R. H.; Raheil, L. A. M. *Polymer* **1988**, *29*, 1539.
(27) Khoury, F. D. *Faraday Discuss. Chem. Soc.* **1979**, *68*, 404.
(28) Liu, J. P.; He, T. B. *Macromol. Rapid Commun.* **2001**, *22*, 1340.
(29) Bartczak, Z.; Argon, A. S.; Chohen, R. R.; Kowalewski, T. *Polymer* **1999**, *40*, 2367.
(30) Keith, H. D. *Polymer* **2003**, *44*, 703.
(31) Taniguchi, N.; Kawaguchi, A. *Macromolecules* **2005**, *38*, 4761.
(32) Keith, H. D.; Padden, F. J., Jr.; Lotz, B.; Wittmann, J. C. *Macromolecules* **1989**, *22*, 2230.
(33) Keith, H. D.; Padden, F. J., Jr. *Polymer* **1984**, *25*, 28.
(34) Lotz, B.; Cheng, S. Z. D. *Polymer* **2005**, *46*, 577.
(35) Hoffman, J. D.; Miller, R. L. *Polymer* **1997**, *38*, 3151.
(36) Keller, A.; Sawada, S. *Makromol. Chem.* **1964**, *74*, 190.
(37) Bassett, D. C.; Hodge, A. M. *Proc. R. Soc. London* **1981**, *A377*, 61.
(38) Keith, H. D. *Polymer* **2001**, *42*, 09987.
(39) Lovinger, A. J. *J. Polym. Sci., Polym. Phys. Ed.* **1980**, *18*, 793.

MA7023842